Materials Science Forum
ISSN: 1662-9752, Vol. 1062, pp 366-370
doi:10.4028/p-2kzz01

Submitted: 2021-10-22
Revised: 2022-02-15
Accepted: 2022-03-07
Online: 2022-05-31

Ray-Tracing Simulation Analysis of Effective Penetration Depths on Grazing Incidence Synchrotron X-Ray Topographic Images of Basal Plane Dislocations in 4H-SiC Wafers

Qianyu Cheng[1,a*], Hongyu Peng[1,b], Shanshan Hu[1,c], Zeyu Chen[1,d], Yafei Liu[1,e], Balaji Raghothamachar[1,f] and Michael Dudley[1,g]

[1]Department of Materials Science and Chemical Engineering, Stony Brook University, Stony Brook, NY, USA

[a]qianyu.cheng@stonybrook.edu, [b]hongyu.peng@stonybrook.edu, [c]shanshan.hu@stonybrook.edu, [d]zeyu.chen@stonybrook.edu, [e]yafei.liu@stonybrook.edu, [f]balaji.raghothamachar@stonybrook.edu, [g]michael.dudley@stonybrook.edu

Keywords: 4H-SiC, X-ray topography, ray-tracing simulation, penetration depth

Abstract. Understanding the depth from which contrast from dislocations is still discernible (the effective penetration depth of the X-rays) in grazing-incidence synchrotron monochromatic beam X-ray topography is of great interest as it enables three-dimensional dislocation configuration analysis and accurate density calculations. To this end, systematic analysis has been performed of topographic and ray-tracing simulated contrast of basal plane dislocations with different Burgers vector and line direction combinations, and a universal method to determine the effective penetration depth based on ray tracing has been developed. This study reveals that the observable dislocation contrast depends on the effective misorientation associated with the dislocation modulated by the photoelectric absorption effect. The dislocations with larger effective misorientation tend to have longer projected length and correspondingly deeper effective penetration depths.

Introduction

Synchrotron X-ray topography (XRT) in the grazing incidence geometry is commonly employed for detailed analysis of dislocation configurations and density calculations in 4° off-axis (0001) 4H-SiC wafers [1]. In this geometry, information on defects from within the effective penetration depth is exclusively revealed. Therefore, it is essential to establish a procedure to define this effective penetration depth. Dudley, et al. used the projected lengths of dislocation images on reflection topographs recorded from in a Si crystal to determine the effective penetration depth [2]. It was concluded that photoelectric absorption rather than extinction limited the observed penetration depths. This was found to be consistent with the direct image contrast formation mechanism i.e. wherein diffracted X-rays emanating from the distorted regions surrounding the dislocation (which contribute to the image) diffract kinematically and, as such, do not undergo extinction but rather just photoelectric absorption [3]. Huang, et al. showed that pure orientation contrast [4], using the ray tracing technique enabled much more accurate simulations of defect images [5]. Ishiji, et al. estimated the penetration depth based on the photoelectric absorption experienced by the diffracted X-rays, thereby assuming that those rays did not undergo extinction but rather just absorption [6]. However, only basal plane dislocations (BPDs) with screw segments parallel to the off-cut $[11\bar{2}0]$-direction were evaluated in that study and other BPDs types were not considered. Therefore, a universal method to determine the effective penetration depth for all dislocation types would be of more practical importance.

In this study, BPDs with different Burgers vector and line direction combinations in physical vapor transport (PVT) grown 4° off-axis 4H-SiC crystals have been investigated by synchrotron X-ray grazing-incidence topography in $1\,1\,\bar{2}\,8$ reflection and accompanying ray-tracing simulations [5] incorporating the effects of surface relaxation [7] and absorption [8, 9]. This ray tracing simulation technique is developed based on the mechanism of orientation contrast [4], where the direction of local diffracted X-ray beams is calculated. By projecting the diffracted X-rays onto the recording plate, the image of the dislocation is simulated. The misorientation associated with the presence of a dislocation is therefore revealed as contrast differences on the image due to the superimposition or separation of diffracted X-rays.

Experiment

PVT-grown, 4° off-axis 4H-SiC substrate wafers are characterized by synchrotron monochromatic X-ray in grazing-incidence geometry. The images were recorded from the Si-face using the $1\,1\,\bar{2}\,8$ reflection at an energy of 8.99 keV at Beamline I-BM of the Advanced Photon Source (APS) at Argonne National Laboratory (ANL). The contrast of BPDs with different combinations of Burgers vectors and line directions was also investigated through ray-tracing simulations. The gray value intensities for both topographic and simulated dislocation contrasts were measured using ImageJ [10]. The length of the dislocation is measured from the end of the contrast feature observed at the surface intersection down to the position where the gray value intensity of the dislocation contrast decreases to 1/10 of the maximum (slightly different procedure from Ishiji [6]).

In this paper, we assume that the rays contributing to the dislocation image in the ray tracing simulations do not experience extinction but only absorption. We then carry out ray tracing simulations at different depths below the surface subjecting each such set of diffracted beams to photoelectric absorption. This is repeated until the dislocation contrast is no longer discernible. Subsequently, all these images from different depths below the surface are stacked upon each other to generate the full simulated dislocation image [8, 9], which is then compared to the observed images to determine the Burgers vectors and effective penetration depth.

Results and Discussion

As shown in Fig. 1, the effective penetration depth t can be calculated based on the observable dislocation contrast in the topograph by $t = \mathrm{L} \times \tan 4^{\circ}$, where the projected length L of each dislocation is measured along the off-cut direction of its observable length

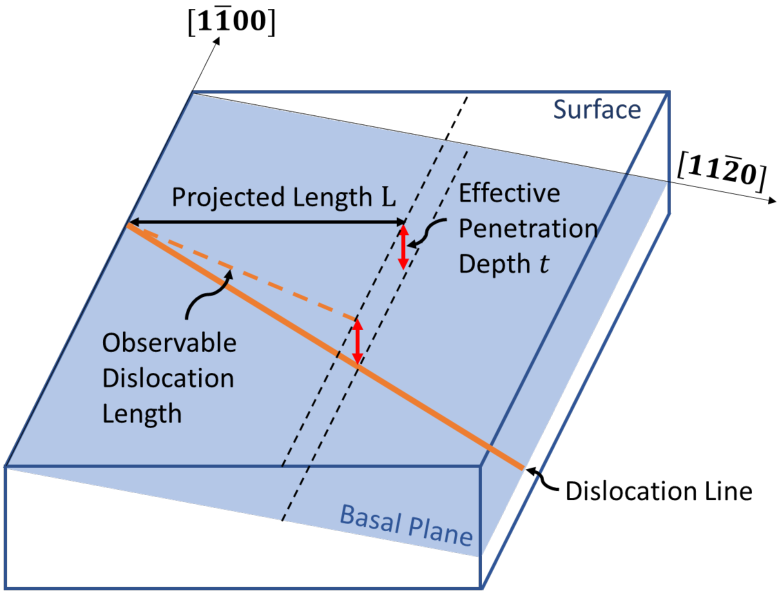

Fig. 1: Schematic diagram of 4° off-axis 4H-SiC. The orange line is a dislocation on the basal plane lying at an arbitrary angle. The dashed orange line represents the observable length of the dislocation on the topograph, and its projected length along off-cut direction is L.

Figure 2 shows four sets of topographic and simulated images of BPDs with different Burgers vector and line direction combinations. The projected lengths measured from each topographic BPD are (from longest to shortest) 207 μm (Fig. 2(a)); 189 μm (Fig. 2(b)); 172 μm (Fig. 2(c)); 87 μm (Fig. 2(d)), corresponding to effective penetration depths of 14.5 μm, 13.2 μm, 12.0 μm, and

6.1 μm, respectively. The Burgers vectors of these dislocations determined by comparing with ray-tracing simulations, are $b = \frac{1}{3}[1\bar{2}10]$, $b = \frac{1}{3}[\bar{1}\bar{1}20]$, $b = \frac{1}{3}[2\bar{1}\bar{1}0]$, and $b = \frac{1}{3}[\bar{2}110]$, respectively. The line directions are measured with respect to their Burgers vectors, which makes them 30° BPD, 30° BPD, 80° BPD, and 0° (screw-type) BPD, respectively. Results clearly indicate that the effective penetration depth varies with the Burgers vector and line direction combination of a dislocation. This effective penetration depth analysis has been conducted for BPDs with all six types of $\frac{1}{3} < 11\bar{2}0 >$ Burgers vector as well as Frank type dislocations created through deflection of threading screw/mixed dislocations onto the basal plane. Those results will be discussed in detail elsewhere [11].

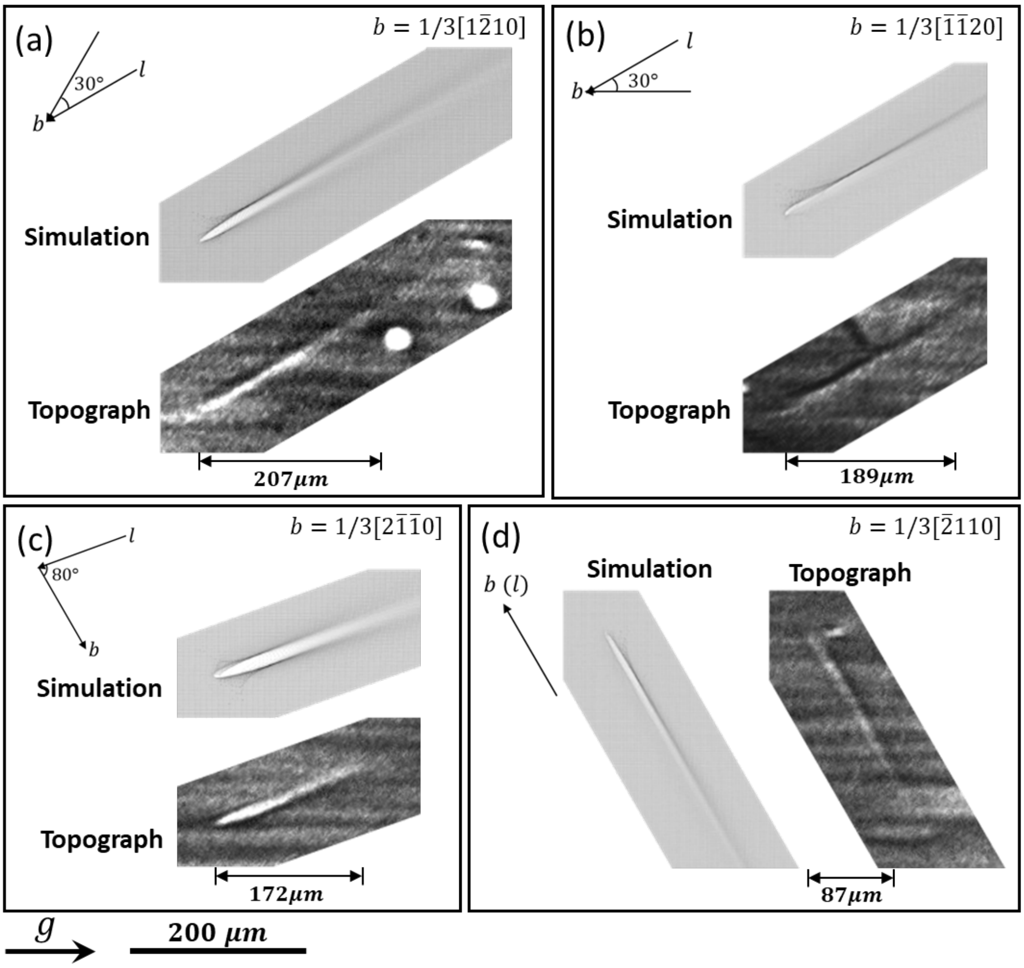

Fig. 2: 1 1 $\bar{2}$ 8 Grazing-incidence X-ray topographs and corresponding ray-tracing simulation results of BPDs with characters of $b = \frac{1}{3}[1\bar{2}10]$, 30° BPD (a); $b = \frac{1}{3}[\bar{1}\bar{1}20]$, 30° BPD (b); $b = \frac{1}{3}[2\bar{1}\bar{1}0]$, 80° BPD (c); $b = \frac{1}{3}[\bar{2}110]$, 0° screw-type BPD (d).

The effective penetration depths obtained through this ray-tracing simulation approach differ from the penetration depth t_0 calculated simply from photoelectric absorption according to Eq. 1:

$$t_0 = \frac{ln10}{\mu(\frac{1}{sin\alpha_0}+\frac{1}{sin\alpha_h})}. \quad (1)$$

where μ is the linear absorption coefficient, α_0 is the incident angle and α_h is the exit angle with the surface. The calculated t_0 is 7.1 μm for 1 1 $\bar{2}$ 8 grazing-incidence topograph at an energy of 8.99 keV. The values calculated using ray tracing differ from this since the strength of the contrast from a dislocation depends on the magnitude of the misorientation and this varies with both line direction and Burgers vector. The stronger the contrast the deeper the effective penetration depth since the starting intensity at the surface intersection is larger and therefore, a fixed value t_0 is insufficient.

While the most accurate and reliable results are found by using ray tracing procedure above, a more simplified model can assist the non-expert in assessing the penetration depth. Since the maximum contrast from a given dislocation is proportional to the local effective misorientation, a measure of this strength can be obtained from an approximate expression for the effective misorientation $\Delta\theta$ as contributed by both the screw and edge components of a dislocation as in Eqs. 2-4:

$$\Delta\theta = |A_1(\boldsymbol{g}\cdot\boldsymbol{b_s})| + |A_2(\boldsymbol{g}\cdot\boldsymbol{b_e})| + |A_3(\boldsymbol{g}\cdot(\boldsymbol{b_e}\times\boldsymbol{l}))|. \quad (2)$$

$$\boldsymbol{b_s} = (\boldsymbol{b}\cdot\boldsymbol{l})\boldsymbol{l}. \quad (3)$$

$$\boldsymbol{b_e} = \boldsymbol{b}\times\boldsymbol{l}\times\boldsymbol{l}. \quad (4)$$

where $\boldsymbol{g}$ is the diffraction vector, $\boldsymbol{b}$ is the Burgers vector, $\boldsymbol{l}$ is the line direction, and $\boldsymbol{b_s}$ and $\boldsymbol{b_e}$ represent the screw and edge components of the Burgers vector, respectively. A_1, A_2, and A_3 are factors calculated based on the lattice displacement of screw and edge dislocation given by Nabarro [12], and are ¼, ¼ and $\frac{1}{4\pi(1-\nu)}$ respectively (ν: Poisson ratio). Detailed descriptions are provided in our upcoming publication [11]. The effective misorientation, $\Delta\theta$, of the dislocations considered here are calculated to be 2.42, 2.18, 1.89, and 0.98. The effective penetration depth t can be estimated through Eq. 5,

$$t = t_0\cdot c\Delta\theta. \quad (5)$$

where c is a constant with an average value around 0.87. For the BPDs shown in Fig. 2, equation 5 yields values of t of 14.9 μm, 13.4 μm, 11.6 μm, and 6.0 μm, respectively. These values are close to those yielded by the full ray tracing simulation approach (14.5 μm, 13.2 μm, 12.0 μm, and 6.1 μm).

Summary

The effective penetration depth of dislocations in grazing-incidence monochromatic beam X-ray topographs in 4° off-cut 4H-SiC wafers is investigated in this study. BPDs with different Burgers vector and line direction combinations are quantitively analyzed in conjunction with ray-tracing simulation incorporating the effects of both surface relaxation and absorption. Analysis of the results indicates that the observable dislocation contrast depends on the effective misorientation associated with the dislocation modulated by the photoelectric absorption effect. As an alternative to the full ray tracing simulation approach, a more simplified factor based on an approximate expression for the effective misorientation (Eqs. 1, 2 and 5) can yield satisfactory results.

Acknowledgements

The information, data, or work presented herein was funded in part by the Advanced Research Projects Agency-Energy (ARPA-E), U.S. Department of Energy, under Award Number DE-AR0001028. The views and opinions of authors expressed herein do not necessarily state or reflect those of the United States Government or any agency thereof. Research used resources of the Advanced Photon Source (Beamline 1-BM), a U.S. Department of Energy (DOE) Office of Science User Facility operated for the DOE Office of Science by Argonne National Laboratory under Contract No. DE-AC02-06CH11357. The Joint Photon Sciences Institute at SBU provided additional support for travel and subsistence at the Advanced Photon Source.

References

[1] B. Raghothamachar, M. Dudley, and G. Dhanaraj, X-ray topography techniques for defect characterization of crystals, in: G. Dhanaraj, K. Byrappa, V. Prasad, and M. Dudley (Eds.), Springer Handbook of Crystal Growth, Springer, Berlin, Heidelberg, 2010, pp. 1425–1451.

[2] M. Dudley, J. Wu, and G.-D. Yao, Nucl. Inst. & Meth. B40/41 (1989) 388-392.

[3] A. Authier, Adv. X-Ray Anal. 10 (1966) 9-31.

[4] M. Dudley, X.-R. Huang, and W. Huang, J. Phys. D: Appl. Phys. 32 (1999) A139-A144.

[5] X.-R. Huang, M. Dudley, M. Vetter, W. Huang, W. Si, and C.-H. Jr Carter, J. Appl. Cryst. 32 (1999) 516-524.

[6] K. Ishiji, S. Kawado, Y. Hirai, and S. Nagamachi, Jpn. J. Appl. Phys. 56 (2017) 106601.

[7] H. Peng, T. Ailihumaer, F. Fujie, Z. Chen, B. Raghothamachar, and M. Dudley, J. Appl. Cryst. 54 (2021) 439-443.

[8] F. Fujie, H. Peng, T. Ailihumaer, B. Raghothamachar, M. Dudley, S. Harada, M. Tagawa, and T. Ujihara, Acta Mater. 208 (2021) 116746.

[9] T. Ailihumaer, H. Peng, F. Fujie, B. Raghothamachar, M. Dudley, S. Harada, and T. Ujihara, Mater. Sci. Eng.: B 271 (2021) 115281.

[10] C. Schneider, W. Rasband, and K. Eliceiri, Nat. Methods 9 (2012) 671-675.

[11] Q. Cheng, H. Peng, S. Hu, Z. Chen, Y. Liu, B. Raghothamachar, and M. Dudley, to be submitted.

[12] F. Nabarro, Theory of Crystal Dislocation, Dover ed., New York, 1987.